

Article

Parameter Optimization and Experiment of a Seed Furrow Cleaning Device for No-Till Maize Seeding

Panpan Yuan ^{1,2,3}, Hongwen Li ^{1,4,*}, Shenghai Huang ^{1,4}, Shan Jiang ^{1,4}, Jing Xu ¹, Han Lin ^{1,4} 
and Rongrong Li ^{1,4}

¹ College of Engineering, China Agricultural University, Beijing 100083, China

² College of Mechanical and Electrical Engineering, Xinjiang Agricultural University, Urumqi 830052, China

³ Key Laboratory of Intelligent Agricultural Equipment, Xinjiang Uygur Autonomous Region, Urumqi 830052, China

⁴ Key Laboratory of Agricultural Equipment for Conservation Tillage, Ministry of Agricultural and Rural Affairs, Beijing 100083, China

* Correspondence: lhwen@cau.edu.cn; Tel.: +86-010-6273-7300

Abstract: To avoid the issues of seeds lying atop straw, where the seeds cannot germinate, during no-till maize seeding, a seed furrow cleaning device is proposed. The device uses rotating spring teeth and a curved sliding shovel to clear the straw from the seed furrow to the outside. The critical components of the side throwing mechanism, rotary disc and spring teeth design are analyzed, and the value range of the installation inclination angle, rotating speed and bending angle of spring teeth are determined. The force on the straw at the moment of starting to touch and throw it is analyzed theoretically in the three installation directions of forward inclination, radial and backward inclination on the rotary disc, and the backward inclination of the spring teeth is determined. A simulation model of the seed furrow cleaning device is established by using the discrete element method simulation software; the forwarding speed, rotating speed, installation inclination angle, and bending angle of spring teeth are used as influencing factors to carry out single-factor experiments. The influence characteristics of different parameters on seed ditch cleaning effect are analyzed from the aspects of straw cleaning quantity and soil disturbance. A field validation experiment is carried out, and the results show that when rotating speed is 180 r/min, installation inclination angle of spring teeth is 40°, and bending angle is 30°, the straw cleaning rate is 82.26%. The research could provide references to develop the no-till seeder for maize seeding.

Keywords: no-till seeding; maize straw; seed furrow cleaning; discrete element method



Citation: Yuan, P.; Li, H.; Huang, S.; Jiang, S.; Xu, J.; Lin, H.; Li, R. Parameter Optimization and Experiment of a Seed Furrow Cleaning Device for No-Till Maize Seeding. *Agriculture* **2022**, *12*, 1901. <https://doi.org/10.3390/agriculture12111901>

Academic Editors: Francesco Marinello and Jacopo Bacenetti

Received: 28 September 2022

Accepted: 8 November 2022

Published: 11 November 2022

Publisher's Note: MDPI stays neutral with regard to jurisdictional claims in published maps and institutional affiliations.



Copyright: © 2022 by the authors. Licensee MDPI, Basel, Switzerland. This article is an open access article distributed under the terms and conditions of the Creative Commons Attribution (CC BY) license (<https://creativecommons.org/licenses/by/4.0/>).

1. Introduction

No-till seeding is carried out by seeding and fertilizing unploughed cropland after harvesting [1,2]. This method can reduce wind and water erosion and improve soil fertility and drought resistance. During the no-till seeding process, the ground remains covered by the previous crop straw [3–6]. When the moisture content of straw is high or straw quantity is large, some straws cannot be cut by the stubble discs, which are pressed into the seed furrow. The straw that is distributed in the seed furrow will seriously affect seeding quality [7] since seeds on top of the straw cannot make contact with the soil. The operation environment is complicated and it is important to clear the furrow of straw before seeds fall in, to provide a clean working environment for seed implantation.

Currently, much research has been carried out on no-till surface straw clearing and planting operations to prevent blockage, mainly including straw self-flow, disc gravity cutting and stubble breaking, and power-driven anti-blocking methods [8–13]. Straw self-flow is a method to increase the straw flow space or accelerate the straw flow by increasing frame beam, improving ground gap, optimizing furrow opener, or adding a straw cleaning mechanism [14–17]. These measures reduce the interaction between straw and seeding

components, and thus promote the smooth passage of straw from both sides of the seeding parts, reduce straw accumulation, and avoid straw stubble blocking at the seeding position. Disc gravity stubble breaking is driving the stubble breaking disc into the soil and rolling it to cut the straw with the stubble using the gravity of the machine [18–22], which requires a considerable positive pressure. This type of seeder is heavy, and the traction method is mostly adopted. The shape and structure of the cutting disc mainly includes a notched disc, corrugated disc, flat disc, concave disc and combined disc [23–25]. The power-driven anti-blocking technology uses high-speed rotating parts to pick up, crush, throw or actively displace the straw in the seeding belt [26–28]. The displaced straws are covered between the seeding rows, creating a good environment without straws for seeding; however, the drawback is that the power consumption of this type of machine is high [29]. The above studies are mainly focused on straw clearing from the surface seeding zone. There are few studies on clearing of the pressed straw in the seed furrow, which would directly affect the emergence rate of seeds.

Based on the above problems, a no-till seed furrow clearing device is proposed in this study for the complex working environment and clearing requirements in the seed furrow during no-till maize seeding. In this study, rotating spring teeth are used to clear the straw from the seed furrow to the outside. The influence of the installation inclination angle and the rotation speed of the spring teeth on the operation effect are analyzed. Meanwhile, the clearing rate of the seed furrow under different parameters and the disturbance to the seed furrow are simulated and analyzed using the discrete element method (DEM). The key parameters are optimized and verified through field experiments. The research provides references to develop a no-till seeder in northwestern regions of China.

2. Materials and Methods

2.1. Mechanized No-Till Seeding of Maize

2.1.1. Process Route

Maize no-till seeding needs to complete a series of procedures, such as applying base fertilizer, clearing the surface straw, opening a seed furrow, seeding, and covering and consolidating soil. The existing maize no-till seeders do not perform seed furrow clearing. Therefore, in view of the special soil environment and agronomic requirements in northwest China, a seed furrow clearing device was added to the conventional no-till seeder to clear off the straw and previous crop residue from the processed seed furrow. The process route of mechanized no-till maize seeding is shown in Figure 1. Each operation link is connected in an orderly manner, and the procedures of applying base fertilizer, clearing surface straw, opening a seed furrow, clearing the seed furrow, seeding, covering and consolidating soil can be completed in one operation.

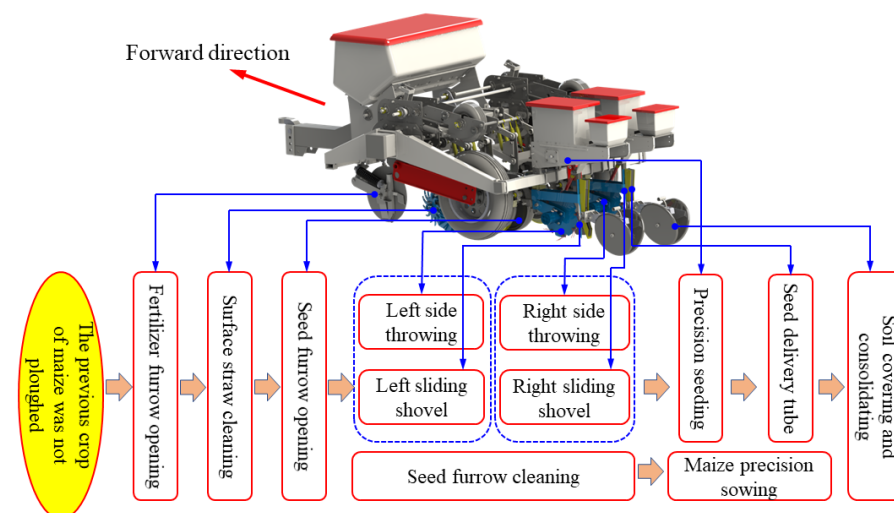


Figure 1. Process route of maize mechanized no-till seeding.

2.1.2. Structure and Working Principle of Maize No-Till Seeder

A maize no-till seeder is composed of traction mechanism, fertilization mechanism, double disc furrow opener, seed metering device, seed furrow clearing device, soil covering and consolidating device, and transmission device. The overall structure of a maize no-till seeder is shown in Figure 2. The surface straw clearing mechanism, furrow opener, seed furrow cleaning device, seed delivery tube, covering and consolidating device are sequentially installed on the no-till seeder unit.

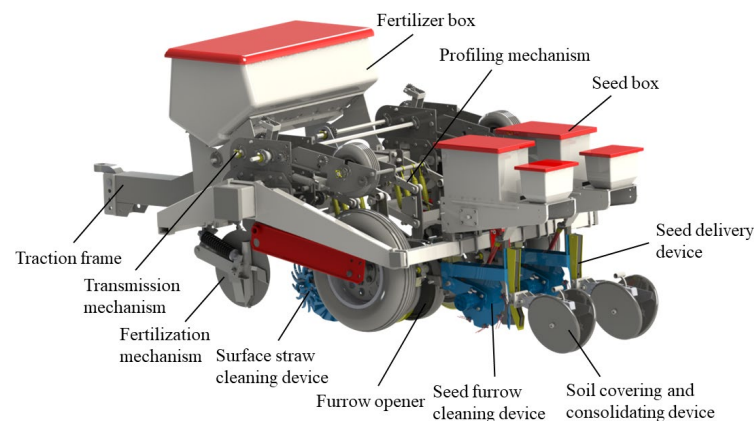


Figure 2. Structure of maize no-till seeder.

The maize no-till seeder is mounted on a tractor and pulled. Firstly, the fertilization disc is used to open the furrow, and fertilizers are applied to the soil by the fertilization mechanism. Secondly, the previous maize surface straws are cleared to both sides by the surface straw clearing mechanism, and the double disc furrow opener processes seed furrow on the cleared seeding belt. Thirdly, the seed furrow clearing device clears the straw. Finally, the seeds fall into the cleared seed furrow and are covered and consolidated.

2.2. Parameter Design of the Seed Furrow Clearing Device

The structure of the seed furrow clearing device is shown in Figure 3. The seed delivery tube, soil covering and consolidating wheel are installed at the rear of the seed furrow clearing device. The spring teeth are uniformly distributed on the rotary disc and rotated with it. A hydraulic cylinder is used to control the height of spring teeth from the ground. The height of the curved sliding shovel is measured by adjusting the fastening bolts to keep the height consistent with the spring teeth. Meanwhile, the rotating speed of spring teeth is controlled by the flow speed control valve. The rotary disc and spring teeth are driven by the hydraulic motor. Under the action of centrifugal force, the straw in the seed furrow is thrown out. Moreover, the curved sliding shovel is used to slide and prevent straw from falling into the cleared seed furrow.

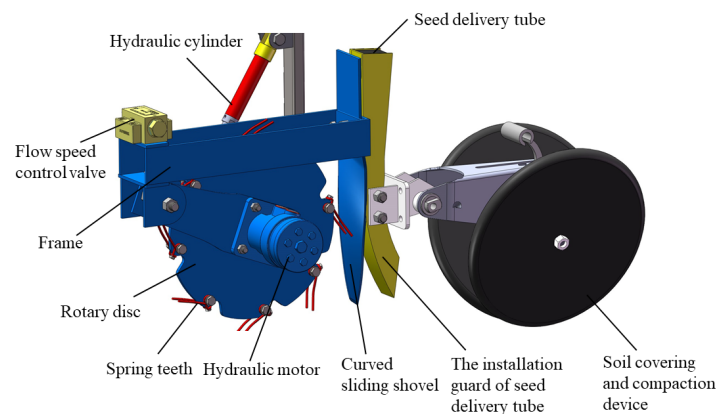


Figure 3. Structural diagram of seed furrow clearing device.

2.2.1. Throwing Mechanism

As shown in Figure 4, the throwing mechanism is composed of rotary disc, flange, hydraulic motor, spring teeth, and adjustment bolts, which complete the actions of picking up, carrying, guiding, and throwing the straw to the outside. In the axial and top two directions, the spring teeth and the rotary disc are fastened by bolts, the top threaded hole is arranged in the circumferential direction of the rotary disc edge arc, and the axial hole is arranged in the axial plane of the rotary disc edge, which effectively prevents relative slippage.

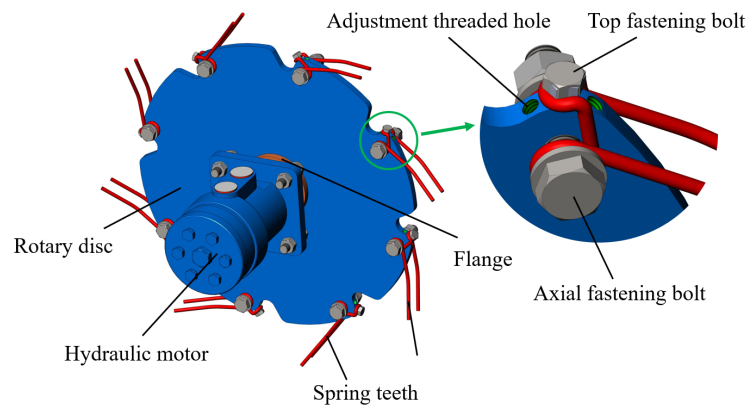


Figure 4. Structural diagram of side throwing mechanism.

The installation inclination angle between the spring teeth and the rotary disc affects the clearing effect of the seed furrow. Three top fastening thread holes are set in the arc circumference direction of the disc edge. The installation inclination angle of spring teeth is adjusted by adjusting the installation position of the top fastening bolts and the threaded hole. As shown in Figure 5, the installation inclination angles are 20° , 40° and 60° , respectively.

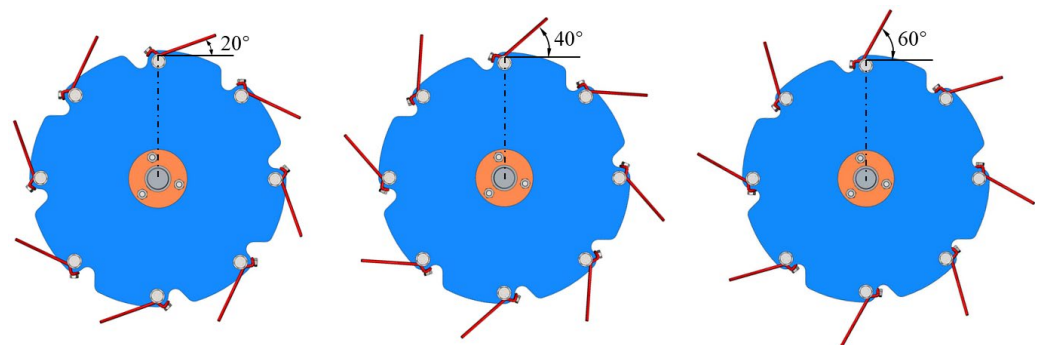


Figure 5. Schematic diagram of different installation inclination angles.

During seed furrow clearing, the interaction between spring teeth and straw requires four stages. The movement process of these stages is shown in Figure 6 and can be described as:

a-b Picking up stage: This is the most critical process of seed furrow clearing. The spring teeth contact and move the straw at a certain speed and insert it into the gap between the straw and the soil, then pick up the straw, simultaneously, give a certain acceleration to the straw.

b-c Carrying and conveying stage: This process carries the straw to the position of throwing. If the rotation speed is too low or the number of spring teeth or the installation inclination angle of the spring teeth is not appropriate, the straw will slip and fall back into the seed furrow.

c-d Throwing stage: Under centrifugal force and self-gravity, the straw is thrown to the outside. This process determines whether the straw can be separated from the spring teeth in time as well as the position where the straw is thrown. If the rotation speed of spring teeth is low, the straw is not thrown out in time, which will carry the straw to the hollow travel stage.

d-a Hollow travel stage: The process of straw being thrown and the next straw being picked up.

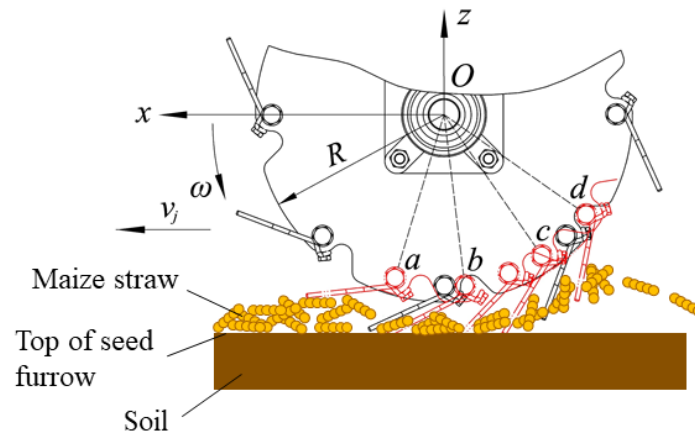


Figure 6. The movement process of seed furrow clearing. The functions of *a–d* are described in the text. Note: *a* is the critical point to touch maize straw; *b* is the critical point to contact soil; *c* is the point to leave soil; *d* is the critical point to throw away; ω is the angular velocity of the spring teeth, rad/s; R is the radius of rotary disc, mm.

2.2.2. Rotary Disc

The edge of the rotary disc has some arcs, which are used to install the spring teeth at the arc space. The structure and parameters of the arc match the structure and size of the spring teeth and correspond to the number of spring teeth. Three top fastening thread holes are machined at the arc position of the disc edge to adjust the installation inclination angle of spring teeth. The thickness of the rotary disc is 10 mm to ensure the processing size and working intensity of the top fastening thread holes. The axial hole is machined at the plane position of the disc edge. The structure and parameters of the rotary disc are shown in Figure 7.

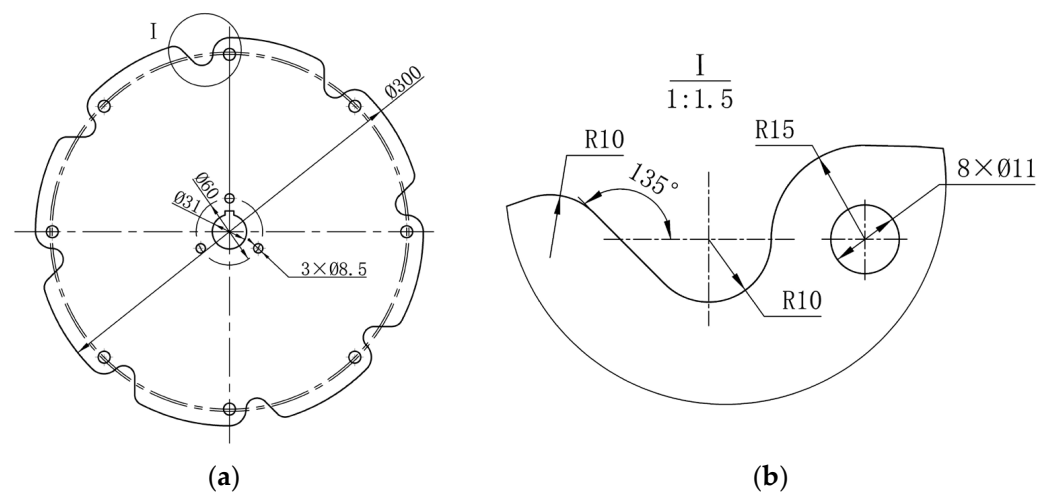


Figure 7. Structural diagram of rotary disc. (a) Front view; (b) Partial enlarged view.

2.2.3. Spring Teeth

The parameters of the spring teeth affect the picking up and throwing trajectory of the straw. As shown in Figure 8, the spring teeth are mainly composed of fixed end, spring teeth spiral and rod, wherein the spring teeth fixed end is composed of axial and top fixing end, spring teeth bar is composed of a straight segment and a bent segment. According to relevant research, the diameter of the spring teeth is 6 mm [30].

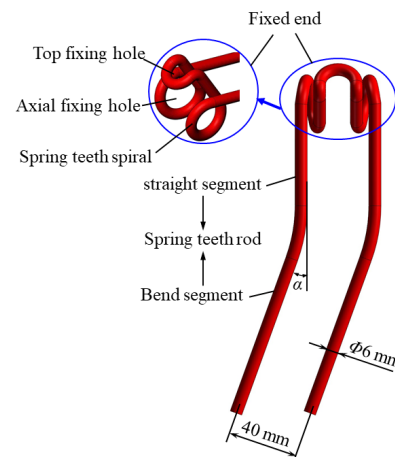


Figure 8. Structure diagram of spring teeth.

The number of spring teeth distributed in the circumferential direction affects the quality of seed furrow clearing. To ensure that the spring teeth can continuously stir and throw the straw without omitting areas, Equation (1) is used to calculate the number of spring teeth distributed on the rotary disc according to the requirements of the agricultural machinery design manual.

$$n = \frac{2\pi(R - l)}{s} \quad (1)$$

where, n is the number of spring teeth; s is the chord length of adjacent spring teeth, mm; l is the effective working length of spring teeth, mm.

According to Equation (1), the number of spring teeth is related to the radius of rotary disc R and the effective working length l of spring teeth.

The circumferential velocity of the spring teeth is as follows:

$$v = R\omega \quad (2)$$

where, v is the circumferential velocity of the spring teeth, m/s.

$$\lambda = \frac{v}{v_j} = \frac{R\omega}{v_j} \quad (3)$$

where, λ is the velocity ratio.

To meet the clearing conditions of straw in the seed furrow, $\lambda > 1$ is required. During the clearing process, the motion trajectory of each point on the spring teeth is a cycloid, and a buckle is formed on the cycloid, as shown in Figure 9. The larger the λ is, the larger the buckle will be. When $\lambda = 1$, it is the critical value of the disappearance of the buckle. To ensure the normal clearing of spring teeth, the rotating speed is required to be greater than the forwarding speed of the seed furrow clearing device. The forwarding speed v_j of the no-till seeder is generally 4~10 km/h; therefore, $R = 150$ mm, 175 mm, and 200 mm, $n = 120$ r/min, 150 r/min, and 180 r/min are substituted into Equation (3), respectively. The calculation shows that the speed ratio of straw clearing λ is greater than 1, and the above parameters meet the normal operating conditions.

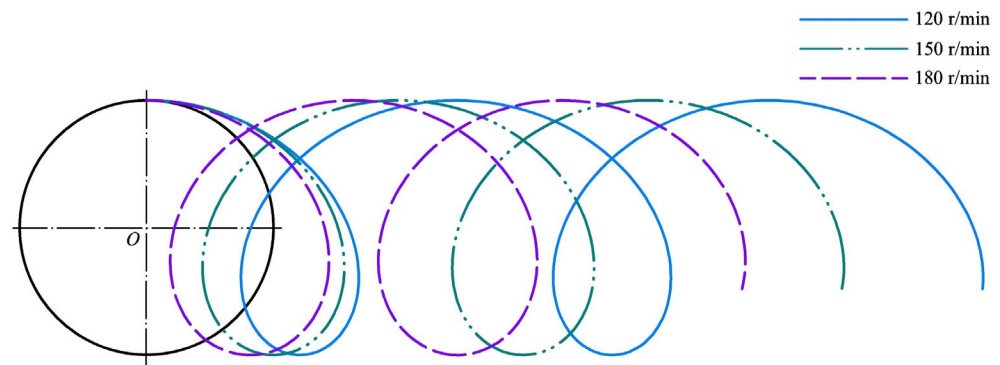


Figure 9. Motion trajectory of spring teeth at different speeds.

As shown in Figure 9, when the forwarding speed v_j is a constant value, the motion trajectories of the spring teeth are different at different speeds. With increased rotating speed, the velocity ratio λ increases, and the maximum transverse chord increases, which indicates that the operation effect will be better.

2.2.4. Installation Direction of Spring Teeth

The straw is not only picked up and thrown out, but also must smoothly fall off of the spring teeth. The installation direction of the spring teeth on the rotary disc affects the clearing effect of straw, as well as the speed of straw after throwing, and then affects the distance of throwing. Along the forward direction of the no-till seeder are three main installation directions of spring teeth: radial, forward and backward inclination.

The diameter of maize straw is generally 15~30 mm, which is smaller than the rotary radius of the spring teeth. Therefore, for this analysis, the maize straw is simplified as particles. The force of maize straw is analyzed when the straw is touched and thrown by the spring teeth in forwarding, radial, and backward inclination. The force analysis of straw at the moment when spring teeth start to touch under three installation types is shown in Figure 10. The coordinate system is established with the straw center as the coordinate origin O , parallel to the forward direction of the machine is the x -axis, and vertical to the ground direction is the y -axis.

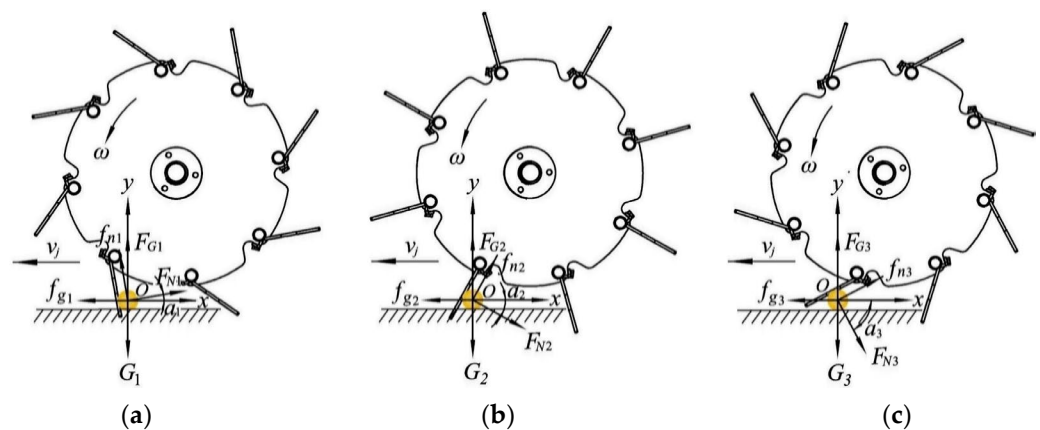


Figure 10. Force analysis of straw at the moment when spring teeth start to touch under three installation types. (a) Forward inclination; (b) Radial; (c) Backward inclination. Note: G_1 , G_2 and G_3 are the gravity of maize straw under the three installation types, respectively, N ; F_{N1} , F_{N2} and F_{N3} are the thrust of spring teeth on maize straw when they are picked up, respectively, N ; F_{G1} , F_{G2} and F_{G3} are the supporting forces of the ground to maize straw respectively, N ; f_{g1} , f_{g2} and f_{g3} are the friction between the ground and maize straw, respectively, N ; f_{n1} , f_{n2} and f_{n3} are the friction between the spring teeth and maize straw, respectively, N ; α_1 , α_2 , and α_3 are the included angles between the thrust F_{N1} , F_{N2} , F_{N3} , and the x -axis, $^\circ$.

When the spring teeth start to touch the straw, the straw has no movement relative to the ground in the vertical direction. That is, the force of the maize straw is balanced in the vertical direction.

$$\begin{cases} F_{G1} + f_{n1} \cos \alpha_1 + F_{N1} \sin \alpha_1 = G_1 \\ F_{G2} + f_{n2} \cos \alpha_2 = G_2 + F_{N2} \sin(-\alpha_2) \\ F_{G3} + f_{n3} \cos \alpha_3 = G_3 + F_{N3} \sin(-\alpha_3) \end{cases} \quad (4)$$

Then

$$\begin{cases} F_{G1} = G_1 - F_{N1} \sin \alpha_1 - f_{n1} \cos \alpha_1 \\ F_{G2} = G_2 - F_{N2} \sin \alpha_2 - f_{n2} \cos \alpha_2 \\ F_{G3} = G_3 - F_{N3} \sin \alpha_3 - f_{n3} \cos \alpha_3 \end{cases} \quad (5)$$

The maize straw has a forward rolling trend along the ground. Thus, the velocity of the straw in the horizontal direction is determined by the resultant force in the horizontal direction. The resultant force in the horizontal direction of the spring teeth under three installation types is as follows:

$$\begin{cases} F_{sx1} = F_{N1} \cos \alpha_1 - f_{n1} \sin \alpha_1 - f_{g1} \\ F_{sx2} = F_{N2} \cos \alpha_2 + f_{n2} \sin \alpha_2 - f_{g2} \\ F_{sx3} = F_{N3} \cos \alpha_3 + f_{n3} \sin \alpha_3 - f_{g3} \end{cases} \quad (6)$$

where, F_{sx1} is the horizontal resultant force when the straw is touched by forwarding inclination spring teeth, N; F_{sx2} is the horizontal resultant force when the straw is touched by radial spring teeth, N; F_{sx3} is the horizontal resultant force when the straw is touched by backward spring teeth, N.

As

$$\begin{cases} f_g = \mu_g F_G \\ f_n = \mu_n F_N \end{cases} \quad (7)$$

where, μ_g, μ_n are the friction coefficient between maize straw and ground, maize straw and spring teeth, respectively.

Equation (7) is substituted into Equation (6).

$$\begin{cases} F_{sx1} = F_{N1} \cos \alpha_1 - \mu_n F_{N1} \sin \alpha_1 - \mu_g (G_1 - F_{N1} \sin \alpha_1 - \mu_n F_{N1} \cos \alpha_1) \\ F_{sx2} = F_{N2} \cos \alpha_2 + \mu_n F_{N2} \sin \alpha_2 - \mu_g (G_2 - F_{N2} \sin \alpha_2 - \mu_n F_{N2} \cos \alpha_2) \\ F_{sx3} = F_{N3} \cos \alpha_3 + \mu_n F_{N3} \sin \alpha_3 - \mu_g (G_3 - F_{N3} \sin \alpha_3 - \mu_n F_{N3} \cos \alpha_3) \end{cases} \quad (8)$$

Let Equation (8) be the following function

$$y_s = F_N \cos \alpha - \mu_n F_N \sin \alpha - \mu_g (G - F_N \sin \alpha - \mu_n F_N \cos \alpha) \quad (9)$$

It can be obtained by deriving Equation (9)

$$\begin{aligned} y_s' &= -F_N \sin \alpha - \mu_n F_N \cos \alpha + \mu_g F_N \cos \alpha - \mu_n \mu_g \sin \alpha \\ &= -(1 + \mu_n \mu_g) F_N \sin \alpha - (\mu_n - \mu_g) F_N \cos \alpha \end{aligned} \quad (10)$$

It can be realized from Figure 10 that the included angle between the thrust of spring teeth on maize straw and the x -axis is $\alpha < 90^\circ$, then the equation $y_s' < 0$ can be obtained, with the increase of angle α , and y_s' decreases. Meanwhile, $\alpha_1 < \alpha_2 < \alpha_3$, so, $F_{sx1} > F_{sx2} > F_{sx3}$ can be obtained. That is, when the spring teeth start to touch the straw under the three installation types, the movement trend of the straw in the horizontal direction is the forward inclination > radial > backward inclination.

The force analysis of straw when spring teeth throw straw under three installation types is shown in Figure 11. Perpendicular to the spring teeth direction is the x -axis, and parallel to the spring teeth direction is the y -axis. When the straw is thrown, the straw leaves the ground, so the ground has no force on the straw, and the straw is only affected by gravity and the force of the spring teeth on the straw.

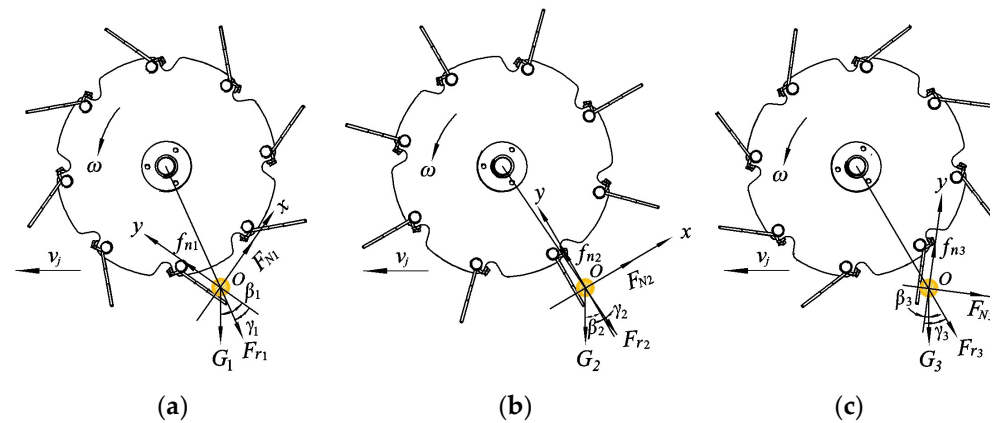


Figure 11. Force analysis of straw when spring teeth throw straw under three installation types. (a) Forward inclination; (b) Radial; (c) Backward inclination. Note: β_1, β_2 and β_3 are the included angles between the gravity of maize straw G_1, G_2, G_3 , and the y -axis, $^\circ$; F_{r1}, F_{r2} and F_{r3} are the centrifugal force of maize straw, N; γ_1, γ_2 and γ_3 are the included angles between the centrifugal force of maize straw F_{r1}, F_{r2}, F_{r3} , and the y -axis, $^\circ$.

The force of the straw is balanced along the contact surface of spring teeth, so the velocity of the straw when spring teeth throw it is determined by the resultant force in the horizontal direction. The resultant force in the horizontal direction of the spring teeth under three installation types is as follows:

$$\begin{cases} F_{tx1} = F_{N1} - G_1 \sin \beta_1 - F_{r1} \sin \gamma_1 \\ F_{tx2} = F_{N2} - G_2 \sin \beta_2 + F_{r2} \sin \gamma_2 \\ F_{tx3} = F_{N3} + G_3 \sin \beta_3 + F_{r3} \sin \gamma_3 \end{cases} \quad (11)$$

where F_{tx1} is the horizontal resultant force when the straw is thrown by forwarding inclination spring teeth, N; F_{tx2} is the horizontal resultant force when the straw is thrown by radial spring teeth, N; F_{tx3} is the horizontal resultant force when the straw is thrown by backward spring teeth, N.

It can be determined from Equation (11) that $F_{tx3} > F_{tx2} > F_{tx1}$, that is, when the straw is thrown under the three installation types, the movement trend of the straw in the horizontal direction is the backward inclination > radial > forward inclination.

According to the above analysis, the forward inclination of the spring teeth is conducive to the action of stirring and picking up the straw, but it has a poor effect on the falling and throwing. The reason is that part of the straw was clumped and could not fall off when thrown at the designated position. However, as the spring teeth continue to rotate, they may fall back into the seed furrow during the rotation process. Therefore, the clearing effect of the seed furrow is affected.

The spring teeth set in the radial direction have a better effect on the straw in working intervals. When the spring teeth rotate at high speed, the straw is easily stirred, picked up, and carried by the spring teeth, but it is also easily thrown into the rear seed furrow, so the side throwing effect is not better.

When the spring teeth are at backward inclination, the stirring of the spring teeth does not affect, and the straw falls off at an appropriate backward angle. In the effective working area, the functions of the spring teeth set backward on the straw is as follows: touching straw, pressing, stirring, picking up, carrying and conveying, falling off, and throwing. Therefore, the spring teeth installation direction is the backward inclination in this study.

2.3. DEM Simulation

2.3.1. Model Materials

The solid model of the maize no-till seed furrow clearing device was established using three-dimensional drawing software, the model of the seed furrow clearing device was

simplified, the parts that were not related to the working process were removed, then STP format was imported into the discrete element simulation software EDEM Geometry item. Considering the simulation efficiency, spherical particles with a radius of 5 mm were selected as soil particles. According to the actual situation of the straw pressed into the seed furrow, a long linear model with a length of 60 mm, which consisted of a diameter of 12 mm, and a spherical center interval of 5 mm was used as the straw particle model. The physical parameters of materials are shown in Table 1, and the basic contact parameters among different materials are shown in Table 2 [31].

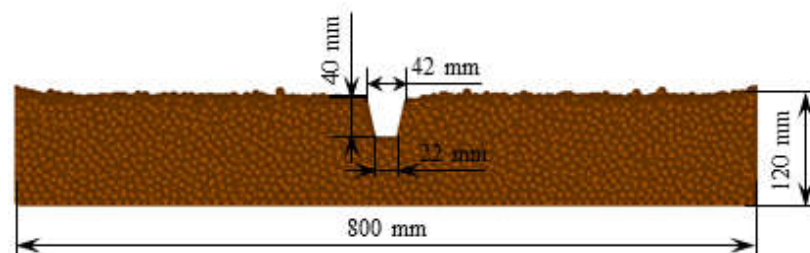
Table 1. Physical parameters of materials.

Object	Poisson's Ratio	Shear Modulus (MPa)	Density (kg/m ³)
soil particle	0.38	1.0×10^6	1850
steel	0.3	7.0×10^{10}	7800
straw	0.4	7.0×10^6	180

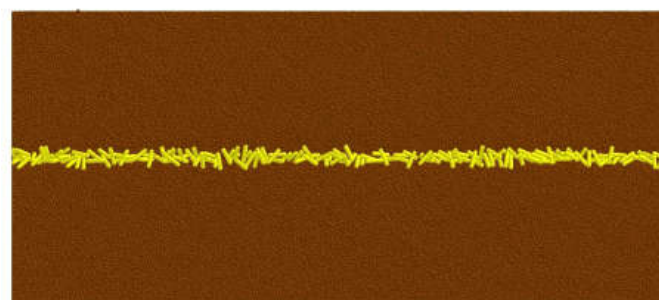
Table 2. Basic contact parameters among different materials.

Object	Soil-Straw	Soil-Soil	Straw-Straw	Steel-Soil	Steel-Straw
Coefficient of restitution	0.5	0.25	0.3	0.28	0.3
Coefficient of static friction	0.3	0.4	0.3	0.5	0.3
Coefficient of rolling friction	0.05	0.25	0.01	0.04	0.01

According to the actual size and operation conditions of the seed furrow, a virtual model of the bin was established in EDEM. The basic dimension (length \times width \times height) of the soil bin was set as 1800 mm \times 800 mm \times 120 mm, and the thickness of the soil layer was 120 mm. As shown in Figure 12, the width of the upper surface of the seed furrow was 42 mm, the width of the bottom was 22 mm, and the depth of the seed furrow was 40 mm. Soil particles fell freely from the grain factory under the action of gravity, so that the simulation environment was as consistent as possible with the actual soil. Maize straws were distributed in the seed furrow, and the straw particles fell freely under the action of gravity.



(a)



(b)

Figure 12. Virtual model of bin. (a) Soil; (b) Soil-straw bin.

The no-till seed furrow clearing device was installed at one end of the soil bin for initial operation. During the operation of the no-till seed furrow clearing device, in order to ensure the continuity of straw and soil particle movement, the total simulation time was set to 2.0 s, and the mesh size was set to 2.5 times the minimum soil particle size.

2.3.2. Test Design and Index Measurement

According to the previous analysis, the main factors of the forwarding speed, rotating speed, installation inclination angle and bending angle of spring teeth were selected, and the influence rules of the above factors on the straw clearing rate and the soil disturbance were analyzed. The forwarding speed of no-till seeder is generally 4~10 km/h, so, the forwarding speeds selected in the test were 4 km/h, 6 km/h and 8 km/h, respectively. According to the previous research [32], the rotating speeds of the spring teeth selected were 120 r/min, 150 r/min, and 180 r/min, respectively. Three top threaded holes were arranged in the circumferential direction of the rotary disc edge arc, and the installation inclination angles were 20°, 40° and 60°, respectively. If the bending angle is too large, the shape of the seed furrow will be damaged; if too small it will not throw the straw out of the seed furrow. According to the pre-experiment, the bending angle was 20°~40°, and the bending angles selected were 20°, 30° and 40° respectively. The single-factor method was conducted, and twelve group experiments were carried out. The single-factor scheme is listed in Table 3.

Table 3. Single-factor simulation scheme.

Number	Factor	Variable Values	Conditions
1–3	Forwarding speed v_j /(km·h ⁻¹)	4, 6, 8	$n = 150 \text{ r} \cdot \text{min}^{-1}$ $\theta = 40^\circ$ $\alpha = 30^\circ$
4–6	Rotating speed n /(r·min ⁻¹)	120, 150, 180	$v_j = 6 \text{ km} \cdot \text{h}^{-1}$ $\theta = 40^\circ$ $\alpha = 30^\circ$
7–9	Inclination angle of spring teeth θ /°	20, 40, 60	$v_j = 6 \text{ km} \cdot \text{h}^{-1}$ $n = 150 \text{ r} \cdot \text{min}^{-1}$ $\alpha = 30^\circ$
10–12	Bending angle of spring teeth α /°	20, 30, 40	$v_j = 6 \text{ km} \cdot \text{h}^{-1}$ $n = 150 \text{ r} \cdot \text{min}^{-1}$ $\theta = 40^\circ$

2.3.3. Data Collection and Processing

1. The straw clearing rate (SCR)

The straw clearing rate is the initial straw quantity minus the remaining quantity in the seed furrow after the operation, and the calculation equation is as follow:

$$\varphi = \frac{N_1 - N_2}{N_1} \times 100\% \quad (12)$$

where, φ is SCR, %; N_1 is initial straw quantity in the seed furrow before operation, pcs; N_2 is remaining straw quantity in the seed furrow after operation, pcs.

2. Soil disturbance quality in seed furrow

During the operation of the seed furrow clearing device, the soil in the seed furrow will be disturbed by the action of the spring teeth and the displacement of the disturbed soil will change. Therefore, soil disturbance quality can be obtained by statistical soil quality changes. A quality sensor was set above the soil surface of the initial seed furrow to monitor the quality of the soil entering the sensor in real-time, that is, the soil disturbance quality.

The simulation process is shown in Figure 13.

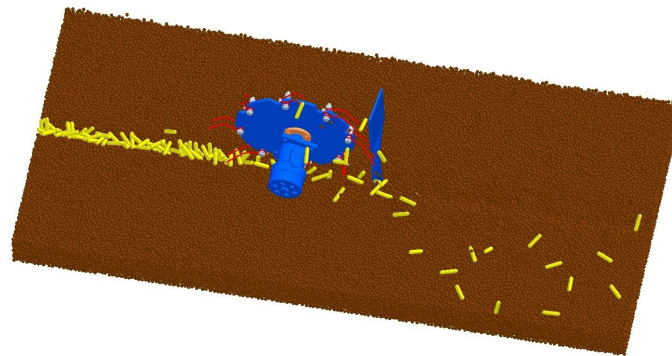


Figure 13. The seed furrow clearing process.

2.4. Field Experiment

The field experiment was conducted in April 2021 at Bole, Xinjiang, China. The soil texture was medium loam, the soil moisture content was 14.35%. The average soil compaction at depth 25 mm was 791 kPa, 50 mm was 1120.8 kPa, and 75 mm was 1283 kPa. The maize straw mulching quantity was 1.64 kg/m². The field experiment is shown in Figure 14.

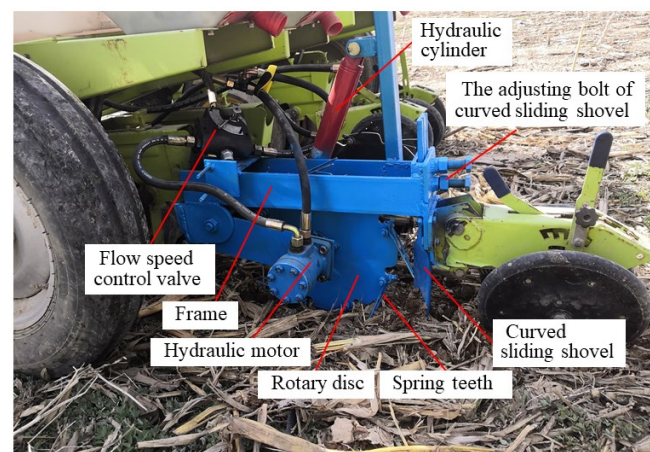


Figure 14. Field experiment of no-till seed furrow clearing device.

3. Results and Discussion

3.1. DEM Simulation Analysis

3.1.1. Seed Furrow Clearing

The changes of straw quantity in the seed furrow under different parameters are shown in Figure 15. With the increase of time, the straw quantity in the seed furrow decreases continuously and then remains stable. This stage is the remaining straw quantity that was not cleared out after the seed furrow was cleared. Figure 15a shows the variation curve of straw quantity in seed furrow under different forwarding speeds. It can be seen that the straw quantity decreases with the increase of forwarding speed, so the SCR improved. The results under different rotating speeds can be seen in Figure 15b. With the increase of the rotating speeds, the SCR increases. Figure 15c shows the effect of different installation inclination angles of the spring teeth on the changes of straw quantity in the seed furrow. With the increase of the installation inclination angle of the spring teeth, the clearing effect of the seed furrow is better. However, when the installation inclination angle is 40° and 60°, the clearing effect of the seed furrow has little difference during 0~0.75 s. Figure 15d shows the variation curve of straw quantity in seed furrow under different bending angles. The straw quantity remaining in the seed furrow decreases with the increase of bending angle.

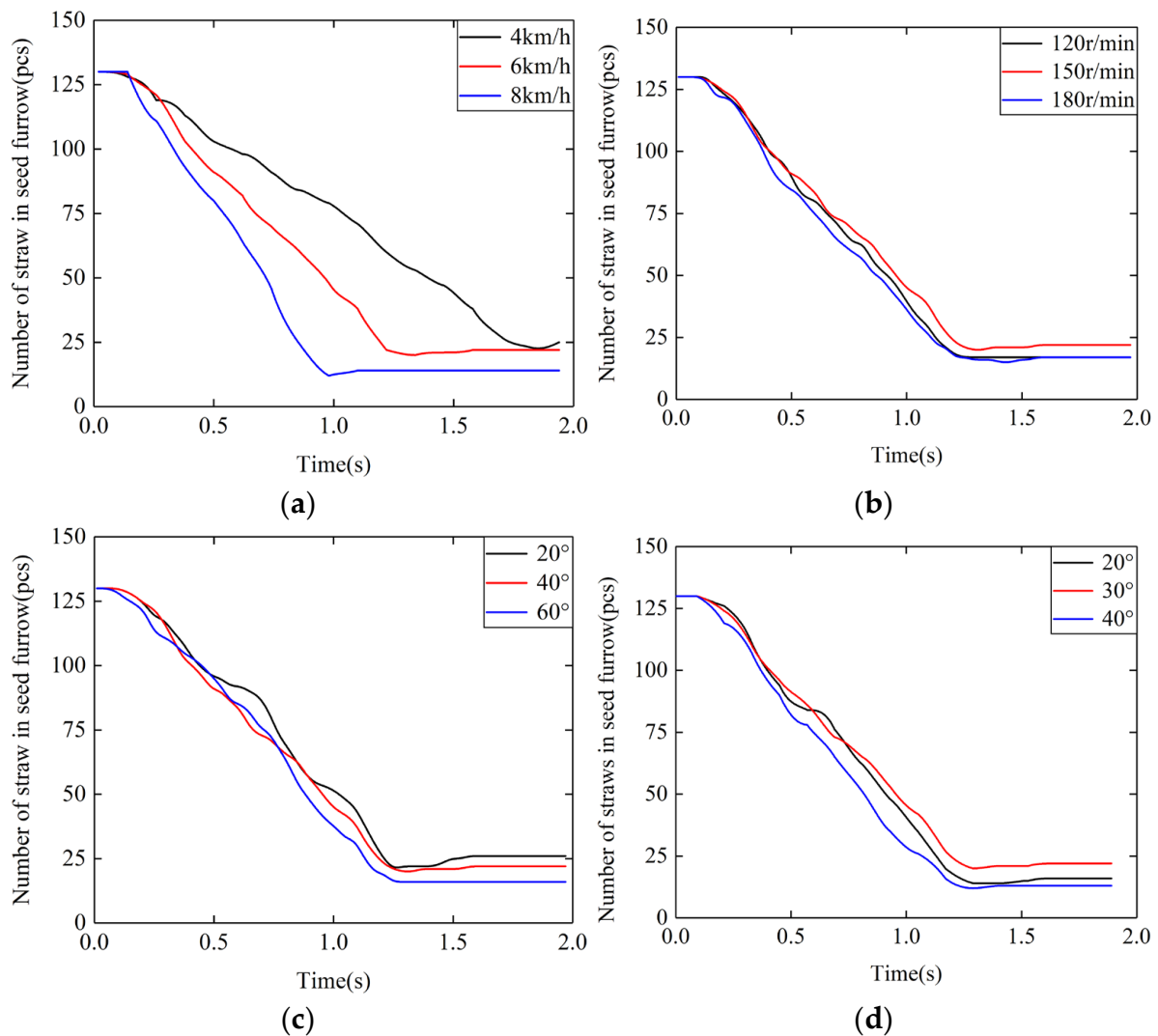


Figure 15. Variation curve of straw quantity in seed furrow clearing under different parameters. (a) Forwarding speed; (b) Rotating speed; (c) Installation inclination angle of spring teeth; (d) Bending angle of spring teeth.

3.1.2. Seed Furrow Soil Disturbance

Soil disturbance affects the original shape of the seed furrow. Hence, in order to maintain the shape of the seed furrow, it is required that the spring teeth have little disturbance to the soil in the seed furrow. The variation curve of soil disturbance in seed furrow clearing under different parameters is shown in Figure 16. It can be seen from Figure 16a that the soil disturbance increases with the decrease of forwarding speed. When $v_j = 4$ km/h, the soil disturbance is the largest, and when $v_j = 6$ km/h and $v_j = 8$ km/h, the soil disturbance is not much different during 0.5~2.0 s. Figure 16b, c shows the variation curve of soil disturbance under different rotating speeds and installation inclination angles, respectively. With the increase of the rotating speeds and installation inclination angle, the soil disturbance increases. Figure 16d shows the variation curve of soil disturbance under different bending angles. When the bending angle $\alpha = 20^\circ$ and $\alpha = 30^\circ$, the variation trend of soil disturbance in the whole operation process is basically the same. When the bending angle $\alpha = 40^\circ$, the soil disturbance is greater than that of the bending angle $\alpha = 20^\circ$ and $\alpha = 30^\circ$ during 0.5~1.0 s, and the variation trend is basically the same in other time periods. Therefore, the change of bending angle has little effect on soil disturbance.

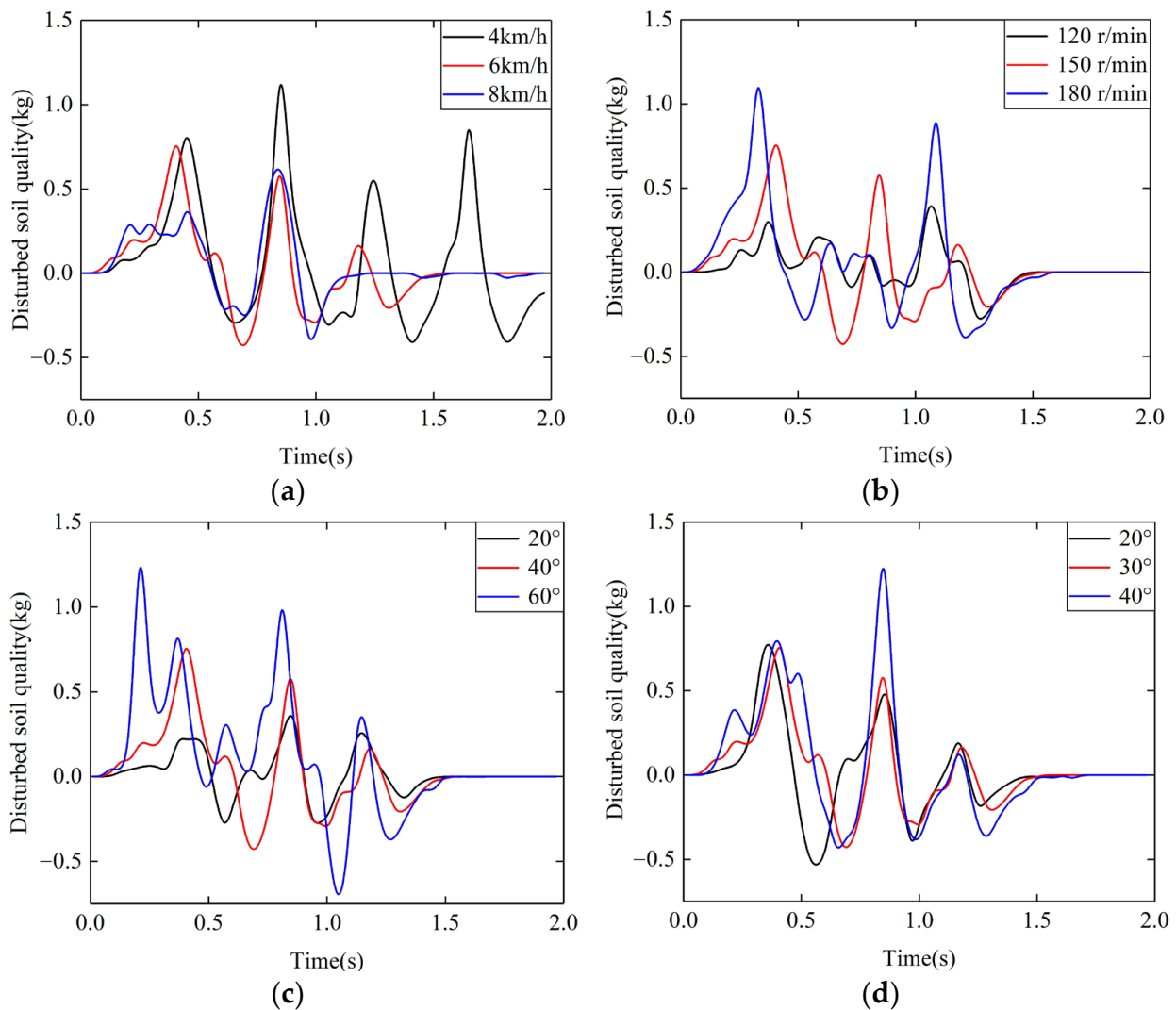


Figure 16. Variation curve of soil disturbance in seed furrow clearing under different parameters. (a) Forwarding speed; (b) Rotating speed; (c) Installation inclination angle of spring teeth; (d) Bending angle of spring teeth.

Therefore, comprehensive straw clearing and soil disturbance evaluation index results are summarized. According to Figures 15a and 16a, with the increase of the forwarding speed, the straw clearing effect is improved, and the soil disturbance is small. Therefore, the forwarding speed is determined to be 8 km/h. With the increase of rotating speed, the straw clearing effect and soil disturbance increases. To obtain better clearing effect, the rotating speed was determined as 180 r/min. With the increase of installation inclination angle, the soil disturbance increased, according to the indicators of straw clearing and soil disturbance, the installation inclination angle was selected as the median value 40°. The change of bending angle had little effect on soil disturbance, according to straw clearing, the bending angle was determined as 30°.

3.2. Field Experiment Analysis

According to the theoretical analysis and simulation results, when the rotating speed of spring teeth was 180 r/min, the installation inclination angle of the spring teeth was 40°, and the bending angle was 30°. The field experiment was conducted. The clearing effect of straw in seed furrow is shown in Figure 17, and the field test results are shown in Table 4.

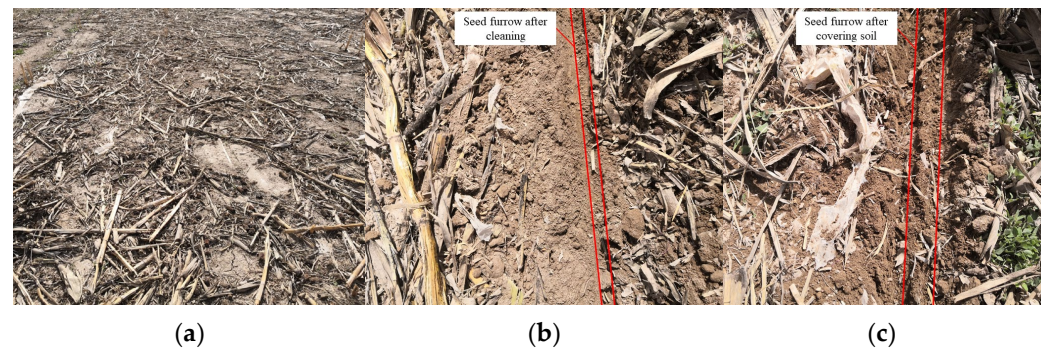


Figure 17. Effect of seed furrow after clearing. (a) Before clearing; (b) Seed furrow after clearing; (c) Seed furrow after covering soil.

Table 4. Field test results of seed furrow clearing effect.

No.	SCR/%
1	73.42
2	85.10
3	92.13
4	74.91
5	82.57
6	89.82
7	71.28
8	80.96
9	90.14
Average	82.26

It can be seen from Table 4 that the average SCR of the seed furrow clearing device was 82.26%. At the same time, the maximum and mean value of throwing distance were measured. The maize maximum value was 314.6 mm. The mean values were 273.4 mm and 117.6 mm, respectively.

4. Conclusions

- (1) A seed furrow clearing device for no-till maize seeding was proposed, which used rotating spring teeth and curved sliding shovel to clear the straw to the outside. The seed furrow was cleared, followed by seeding, covering and consolidating soil.
- (2) The installation directions of the spring teeth on the rotary disc include forward inclination, radial and backward inclination. The force on the straw at the moment of starting to touch and throwing the straw was analyzed theoretically, and the backward inclination of the spring teeth was determined. In the appropriate backward inclination angle, the stirring of the spring teeth would not affect, and the straw would fall off the spring teeth.
- (3) The straw clearing rate and soil disturbance were analyzed by using the DEM method. The results indicated that increases in the forwarding speed, rotating speed, installation inclination angle and bending angle, the straw clearing rate increased, generally. With the increase of the forwarding speed, the straw clearing effect was improved, and the soil disturbance was small, the forwarding speed was determined as 8 km/h. With the increase of the rotating speed, the soil disturbance increased, to obtain better clearing effect, the rotating speed was determined as 180 r/min. With the increase of installation inclination angle, the soil disturbance increased, according to the indicators of straw clearing and soil disturbance, the installation inclination angle was selected as the median value 40°. The change of bending angle had little effect on soil disturbance, according to straw clearing, the bending angle was determined as 30°.

- (4) The field experiment results showed that when the rotating speed was 180 r/min, installation inclination angle of spring teeth was 40°, and bending angle was 30°, the SCR was 82.26%.

Author Contributions: Conceptualization, P.Y.; writing—original draft preparation, P.Y., H.L. (Hongwen Li); writing—review and editing, S.H., S.J., J.X., H.L. (Han Lin), R.L. All authors have read and agreed to the published version of the manuscript.

Funding: This research was funded by the National Natural Science Foundation of China No. 52165039, Xinjiang key research and development program (2022B02025-3), Xinjiang Agricultural Machinery R&D, Manufacturing, Promotion and Application Integration Project (YTHSD2022-14).

Institutional Review Board Statement: Not applicable.

Data Availability Statement: Not applicable.

Acknowledgments: Gratitude should be expressed to all the members of the Conservation Tillage Research Centre.

Conflicts of Interest: The authors declare no conflict of interest.

References

- Chabert, A.; Sarthou, J.P. Conservation agriculture as a promising trade-off between conventional and organic agriculture in bundling ecosystem services. *Agric. Ecosyst. Environ.* **2020**, *292*, 106815. [CrossRef]
- He, J.; Li, H.; Chen, H.; Lu, C.; Wang, Q. Research progress of conservation tillage technology and machine. *Trans. Chin. Soc. Agric. Mach.* **2018**, *49*, 1–19.
- Liu, J.; Li, J.; Zhou, Y.; Fu, Q.; Zhang, L.; Liu, L. Effects of straw mulching and tillage on soil water characteristics. *Trans. Chin. Soc. Agric. Mach.* **2019**, *50*, 333–339.
- Celik, A.; Altikat, S.; Way, T.R. Strip tillage width effects on sunflower seed emergence and yield. *Soil Tillage Res.* **2013**, *131*, 20–27. [CrossRef]
- Nyakudya, I.W.; Stroosnijder, L. Conservation tillage of rainfed maize in semi-arid Zimbabwe: A review. *Soil Tillage Res.* **2015**, *145*, 184–197. [CrossRef]
- Zeng, Z.; Chen, Y. Performance evaluation of fluted coulters and rippled discs for vertical tillage. *Soil Tillage Res.* **2018**, *183*, 93–99. [CrossRef]
- Liu, Z.; Liu, L.; Yang, X.; Zhao, Z.; Liu, X. Design and experiment of no-till precision planter for corn. *Trans. Chin. Soc. Agric. Eng.* **2016**, *32*, 1–6.
- Wang, Q.; Cao, X.; Wang, C.; Li, H.; He, J.; Lu, C. Research progress of no/minimum tillage corn seeding technology and machine in northeast black land of China. *Trans. Chin. Soc. Agric. Mach.* **2021**, *52*, 1–15.
- KUHN Krause Gladiator. Available online: <https://www.kuhn-usa.com/crop/tillage-tools/strip-till> (accessed on 8 September 2022).
- Olaf, E. Cropping systems and crop residue management in the Trans-Gangetic Plains: Issues and challenges for conservation agriculture from village surveys. *Agric. Syst.* **2011**, *104*, 54–62.
- Siemens, M.C.; Wilkins, D.E.; Correa, R.F. Development and evaluation of a residue management wheel for hoe-type no-till drills. *Trans. ASAE* **2003**, *47*, 397–404. [CrossRef]
- Ahmad, F.; Qiu, B.; Ding, Q.; Ding, W.; Khan, Z.M.; Shoaib, M.; Chandio, F.A.; Rehman, A.; Khaliq, A. Discrete element method simulation of disc type furrow openers in paddy soil. *Int. J. Agric. Biol. Eng.* **2020**, *13*, 103–110. [CrossRef]
- Hou, S.; Chen, H.; Zou, Z.; Wei, Z.; Zhang, Y. Design and test of lateral stubble cleaning blade for corn stubble field. *Trans. Chin. Soc. Agric. Eng.* **2020**, *36*, 59–69.
- DALE DRILLS Eco L. Available online: <http://www.daledrills.com/drill-range/eco--drill> (accessed on 8 September 2022).
- John Deere 1705 Twin Row Planter. Available online: <https://www.deere.com/en/planting-equipment/1705-twin-row-planter/#> (accessed on 8 September 2022).
- Zhang, X.; Li, H.; Du, R.; Ma, S.; He, J.; Wang, Q.; Chen, W.; Zheng, Z.; Zhang, Z. Effects of key design parameters of tine furrow opener on soil seedbed properties. *Int. J. Agric. Biol. Eng.* **2016**, *9*, 67–80.
- Yuan, P.; Li, H.; Jiang, G.; He, J.; Lu, C.; Huang, S. Design and experiment of straw cleaning device for wide narrow maize no-tillage sowing strip in drip irrigation area. *Trans. Chin. Soc. Agric. Mach.* **2021**, *52*, 43–52.
- AGCO Sunflower STRIP-TILL TOOLS. Available online: <https://www.sunflowermfg.com/tillage-equipment/strip-till> (accessed on 8 September 2022).
- Sharipov, G.M.; Paraforos, D.S.; Pulatov, A.S.; Griepentrog, H.W. Dynamic performance of a no-till seeding assembly. *Biosyst. Eng.* **2017**, *158*, 75–94. [CrossRef]
- Brandelero, E.M.; Araújo, A.G.D.; Ralisch, R. Coverage mobilization by different no-tillage in-line handling mechanisms. *Eng. Agric.* **2015**, *35*, 89–97. [CrossRef]

21. Vaitauskienė, K.; Šarauskis, E.; Romaneckas, K.; Jasinskas, A. Design, development and field evaluation of row-cleaners for strip tillage in conservation farming. *Soil Tillage Res.* **2017**, *174*, 139–146. [[CrossRef](#)]
22. Boss Engineering Strip till Machines [EB/OL]. Available online: <https://bossagriculture.com.au/home/strip-till-machines> (accessed on 19 October 2022).
23. Silva, P.R.A.; Benez, S.H.; Jasper, S.P.; Seki, A.S.; Masiero, F.C.; Riquetti, N.B. Seedrill: Mechanism of culting straw and applied vertical loads. *Rev. Bras. Eng. Agrícola Ambient.* **2021**, *16*, 1367–1373. [[CrossRef](#)]
24. Wang, Q.; Jia, H.; Zhu, L.; Li, M.; Zhao, J. Design and experiment of star-toothed concave disk row cleaners for no-till planter. *Trans. Chin. Soc. Agric. Mach.* **2019**, *50*, 68–77.
25. Nejadi, J.; Raoufat, M.H. Field performance of a pneumatic row crop planter equipped with active toothed coulter for direct planting of corn in wheat residue. *Span. J. Agric. Res.* **2013**, *11*, 327–334. [[CrossRef](#)]
26. Matin, M.A.; Fielke, J.M.; Desbiolles, J.M.A. Torque and energy characteristics for strip-tillage cultivation when cutting furrows using three designs of rotary blade. *Biosyst. Eng.* **2015**, *129*, 329–340. [[CrossRef](#)]
27. Li, Y.; Lu, C.; Li, H.; He, J.; Wang, Q.; Huang, S.; Gao, Z.; Yuan, P.; Wei, X.; Zhan, H. Design and experiment of spiral discharge anti-blocking and row-sorting device of wheat no-till planter. *Agriculture* **2022**, *12*, 468. [[CrossRef](#)]
28. Zhu, H.; Qian, C.; Bai, L.; Zhao, H.; Ma, S.; Zhang, X.; Li, H. Design and experiments of active anti-blocking device with forward-reverse rotation. *Trans. Chin. Soc. Agric. Eng.* **2022**, *38*, 1–11.
29. Wang, W.; Zhu, C.; Chen, L.; Li, Z.; Huang, X.; Li, J. Design and experiment of active straw-removing anti-blocking device for maize no-tillage planter. *Trans. Chin. Soc. Agric. Eng.* **2017**, *33*, 10–17.
30. Cao, X.; Wang, Q.; Li, H.; He, J.; Lu, C.; Yu, C. Design and experiment of active rotating collective straw-cleaner. *Trans. Chin. Soc. Agric. Eng.* **2021**, *37*, 26–34.
31. Yu, C.; Wang, Q.; Li, H.; He, J.; Lu, C.; Liu, H. Design and Experiment of Spiral-split Sowing Strip Cleaning Device. *Trans. Chin. Soc. Agric. Mach.* **2020**, *51*, 212–219.
32. Yuan, P.; Li, H.; Lu, C.; Wang, Q.; He, J.; Huang, S.; Cui, D. Design and experiment of seed furrow cleaning device based on throwing and sliding for no-till maize seeding. *Int. J. Agric. Biol. Eng.* **2022**, *15*, 95–102. [[CrossRef](#)]